

Interfacial Reactivity of Monolayer-Protected Clusters Studied by Scanning Electrochemical Microscopy

Bernadette M. Quinn,* Peter Liljeroth, and Kyösti Kontturi

Contribution from the Laboratory of Physical Chemistry and Electrochemistry, Helsinki University of Technology, P.O. Box 6100, FIN-02015 HUT, Finland

Received August 20, 2002

Abstract: Solutions of monodisperse monolayer-protected clusters (MPCs) of gold can be used as multivalent redox mediators in electrochemical experiments due to their quantized double-layer charging properties. We demonstrate their use in scanning electrochemical microscopy (SECM) experiments wherein the species of interest (up to 2-electron reduction or 4-electron oxidation from the native charge-state of the MPCs) is generated at the tip electrode, providing a simple means to adjust the driving force of the electron transfer (ET). Approach curves to perfectly insulating (Teflon) and conducting (Pt) substrates are obtained. Subsequently, heterogeneous ET between MPCs in 1,2-dichloroethane and an aqueous redox couple (Ce(IV), $\text{Fe}(\text{CN})_6^{3-/4-}$, $\text{Ru}(\text{NH}_3)_6^{3+}$, and $\text{Ru}(\text{CN})_6^{4-}$) is probed with both feedback and potentiometric mode of SECM operation. Depending on the charge-state of the MPCs, they can accept/donate charge heterogeneously at the liquid–liquid interface. However, this reaction is very slow in contrast to ET involving MPCs at the metal–electrolyte interface.

Introduction

There is considerable current interest in the electronic properties of alkanethiol stabilized metallic nanoparticles, so-called “monolayer-protected clusters” (MPCs),^{1–3} and it has been proposed that assemblies of such MPCs have the potential to form the structural elements for electronic nanodevices. MPCs can store charge, due to a combination of their size and the sub-attofarad capacitance associated with the protecting layer, and can be considered as multivalent redox species.^{3–7} The single electron transfer (ET) characteristics demonstrated by suitably monodisperse MPC fractions of small core size has been termed quantized double layer charging (QDL) and has been observed both for freely diffusing solution species and for MPC films attached to electrodes.^{1,3,8,9} QDL charging has been reported for both metal (Au, Ag, Cu, and Pd) and semiconductor MPCs, although the majority of studies have

concentrated on Au MPCs.^{4,8,10–12} Pioneering work by Murray and co-workers has greatly increased our understanding of the electrochemical properties of MPCs, and it is clear that they can be treated as redox reagents: the charge stored in MPCs can be used to carry out redox reactions with both conventional donor or acceptor molecules and MPCs of different charge. Solutions of MPCs can be electrolytically charged to controllable potentials, and the charged MPCs are stable and can be isolated in solid form.⁵

Rates of electron transfer in different assemblies of MPCs have been studied extensively. For freely diffusing MPCs, electron transfer to the metal core has been shown to be kinetically fast, and the equilibrium or rest potential of the MPC solution can be described in terms of the Nernst equation.^{1,5} In dry, solid-state MPC assemblies, the ET between the nanoparticles has been shown to be very fast and to vary exponentially with the distance between the metal cores.⁷ Studies of nanoparticle films in contact with an electrolyte solution have also yielded high values of the hopping rate constant between the particles.⁶ On the other hand, ET between nanoparticles and the electrode in a carboxylate-divalent metal ion-carboxylate bridged film occurs at a much lower rate (rate constant of $\sim 10^2 \text{ s}^{-1}$).¹³ The same study concluded that the ET takes place through the bonded pathway, and the rate is strongly dependent on the linker chain length. In a report concerning MPCs incorporated in polyelectrolyte multilayers on electrodes, it was demonstrated that the rate of charge transfer was dependent on the nature of

* To whom correspondence should be addressed. E-mail: bquinn@cc.hut.fi. Tel: +358 9 451 2579. Fax: +358 9 451 2580.

- (1) Templeton, A. C.; Wuelfing, W. P.; Murray, R. W. *Acc. Chem. Res.* **2000**, *33*, 27–36.
- (2) Markovich, G.; Collier, C. P.; Henrichs, S. E.; Remacle, F.; Levine, R. D.; Heath, J. R. *Acc. Chem. Res.* **1999**, *32*, 415–423.
- (3) Chen, S.; Ingram, R. S.; Hostetler, M. J.; Pietron, J. J.; Murray, R. W.; Schaaff, T. G.; Khoury, J. T.; Alvarez, M. M.; Whetten, R. L. *Science* **1998**, *280*, 2098–2101.
- (4) Chen, S.; Murray, R. W.; Feldberg, S. W. *J. Phys. Chem. B* **1998**, *102*, 9898–9907.
- (5) Pietron, J. J.; Hicks, J. F.; Murray, R. W. *J. Am. Chem. Soc.* **1999**, *121*, 5565–5570.
- (6) Hicks, J. F.; Zamborini, F. P.; Osisek, A. J.; Murray, R. W. *J. Am. Chem. Soc.* **2001**, *123*, 7048–7053.
- (7) Wuelfing, W. P.; Green, S. J.; Pietron, J. J.; Cliffler, D. E.; Murray, R. W. *J. Am. Chem. Soc.* **2000**, *122*, 11 465–11 472.
- (8) Ingram, R. S.; Hostetler, M. J.; Murray, R. W.; Schaaff, T. G.; Khoury, J.; Whetten, R. L.; Bigioni, T. P.; Guthrie, D. K.; First, P. N. *J. Am. Chem. Soc.* **1997**, *119*, 9279–9280.
- (9) Zamborini, F. P.; Hicks, J. F.; Murray, R. W. *J. Am. Chem. Soc.* **2000**, *122*, 4514–4515.

- (10) Chen, S.; Sommers, J. M. *J. Phys. Chem. B* **2001**, *105*, 8816–8820.
- (11) Cheng, W.; Dong, S.; Wang, E. *Electrochem. Commun.* **2002**, *4*, 412–416.
- (12) Ding, Z.; Quinn, B. M.; Haram, S. K.; Pell, L. E.; Korgel, B. A.; Bard, A. J. *Science* **2002**, *296*, 1293–1297.
- (13) Hicks, J. F.; Zamborini, F. P.; Murray, R. W. *J. Phys. Chem. B* **2002**, *106*, 7751–7757.

monolayer protecting the metal core. Despite not presenting actual values of the rate constant, it was clear that the ionic conductivity of layers consisting of poly(sodium 4-styrene sulfonate) and mercaptophenylamine stabilized Au particles was much higher than in poly(allylamine hydrochloride) and mercaptoundecanoic acid stabilized particles.¹⁴

Another interesting aspect of MPC film electrochemistry is the rectified quantized charging phenomenon.^{15–18} This refers to quantized charging of the nanoparticle layers, which is dependent on the nature of the ions in the bathing solution; in particular, positive charging of the nanoparticle film was facilitated by the presence of hydrophobic anions, which can enter the film to maintain charge neutrality. Similar behavior has been noted earlier with films of buckminster fullerene in aqueous solutions.^{19–21}

As MPCs are tunable redox species, advanced electrochemical techniques such as scanning electrochemical microscopy (SECM) can provide fundamental information concerning the reactivity of differing charge states with substrates of interest.²² SECM is proving to be a powerful means of obtaining reliable kinetic data at an ever increasing variety of interfaces.^{23–27} Recent applications of the technique include the study of lateral proton diffusion in Langmuir monolayers,²⁸ metal–insulator transitions of 2-D nanocrystal films²⁹ and catalytic reactions at underivatized gold nanoparticle films.³⁰ In the majority of SECM studies, the tip microelectrode is operated under amperometric conditions, wherein the redox mediator is electrolyzed at the SECM tip and the resulting tip current is monitored as a function of distance from the substrate under investigation. SECM can also be used in potentiometric mode where the tip is a passive probe, typically an ion-selective electrode that detects the local activity of a given species, e.g., concentration gradients at the substrate.^{31–33} Liu et al. recently demonstrated both amperometric and potentiometric imaging with an Sb tip.³²

Here, we attempt to quantify charge transfer (CT) to the metal core of MPCs and report the novel use of SECM to investigate

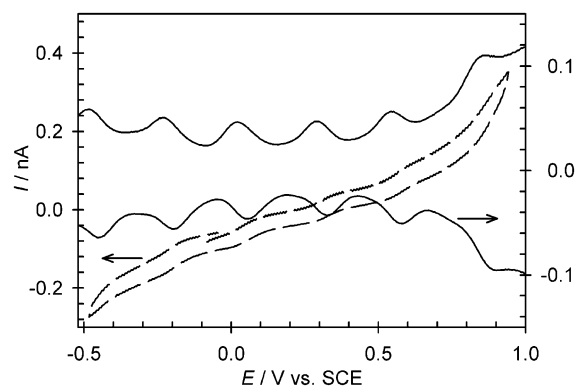


Figure 1. Differential pulse (—) and cyclic voltammetry (---) of Au C6 MPCs (ca. 0.03 mM) illustrating quantized double layer charging.

the kinetics of CT at the metal–electrolyte and liquid–liquid interfaces using the MPCs as the redox species. It is demonstrated that a Pt SECM tip can be used both as an active probe in amperometric mode and as a passive probe in potentiometric mode of SECM operation. In the former mode, different charge states of the MPC are generated at the electrode surface, whereas in the latter, the Pt tip is used as redox reference electrode to follow the equilibrium potential of the MPC solution.

Experimental Section

Chemicals. The aqueous redox species used were $K_3Fe(CN)_6$ (Merck), $K_4Fe(CN)_6$ (Aldrich), $K_2Ru(CN)_6$ (Alfa Aesar), $Ru(NH_3)_6Cl_3$ (Alfa Aesar), and $Ce(SO_4)_2$ (Aldrich). 1,2-Dichloroethane (1,2-DCE) was obtained from Rathburn (UK) and was used as received. Tetraphenylarsonium pentafluorophenyl borate (TPAsTPBF₂₀), tetrabutylammonium pentafluorophenyl borate (TBATPBF₂₀), and tetramethylammonium pentafluorophenyl borate (TMATPBF₂₀) salts were prepared by metathesis of the corresponding chloride TPAsCl (Fluka), TBACl (Aldrich) or TMACl (Fluka) with LiTPBF₂₀ (Boulder Scientific) in a 2:1 mixture of methanol and water. The resulting precipitates were filtered, washed and recrystallized from acetone. All other chemicals were of the highest commercially available purity. Aqueous solutions were prepared using MQ-treated water (Millipore, US).

Nanoparticle Synthesis. Hexanethiolate MPCs (C6 MPCs) were synthesized according to a literature procedure proven to yield MPCs with small core diameters.^{5,34} The crude MPC product was then size selected by fractional precipitation to isolate particles with smaller core diameters.³⁵ Briefly, as prepared MPCs were dispersed in chloroform and an equal volume of a nonsolvent added (acetonitrile). After being stirred overnight, the solution was filtered to remove precipitated larger particles, and the supernatant was rotary evaporated to dryness. The resulting fractions were then cleaned using a dispersion, precipitation, filtration and washing cycle. The various fractions were electrochemically characterized using differential pulse voltammetry (DPV) and cyclic voltammetry (CV) at a 25 μ m Pt ultramicroelectrode (UME), where the particles were dissolved in 10 mM tetrabutylammonium perchlorate (TBAClO₄) DCE solution. The entire procedure was repeated varying the volume ratio of solvent to nonsolvent until an even peak spacing characteristic of reasonable core monodispersity was obtained in DPVs (Figure 1).⁴

Electrochemical Measurements. CV, DPV, and SECM measurements were performed using a commercially available SECM instrument (CHI-900, CH-Instruments, TX). A two-electrode arrangement was used, in which a silver wire was used both as quasi-reference

- (14) Hicks, J. F.; Young, S.-S.; Murray, R. W. *Langmuir* **2002**, *18*, 2288–2294.
 (15) Chen, S. *J. Am. Chem. Soc.* **2000**, *122*, 7420–7421.
 (16) Chen, S.; Pei, R. *J. Am. Chem. Soc.* **2001**, *123*, 10 607–10 615.
 (17) Chen, S.; Pei, R.; Zhao, T.; Dyer, D. J. *J. Phys. Chem. B* **2002**, *106*, 1903–1908.
 (18) Jhaveri, S. D.; Lowy, D. A.; Foos, E. E.; Snow, A. W.; Ancona, M. G.; Tender, L. M. *Chem. Commun.* **2002**, 1544–1545.
 (19) Jehoulet, C.; Bard, A. J.; Wudl, F. *J. Am. Chem. Soc.* **1991**, *113*, 5456–5457.
 (20) Chlistunoff, J.; Cliffel, D.; Bard, A. J. *Thin Solid Films* **1995**, *257*, 166–184.
 (21) Sz^ocs, I. *J. Electroanal. Chem.* **2001**, *505*, 159–164.
 (22) One of the referees has drawn it to our attention that the use of MPCs as SECM mediators has been proposed by David E. Cliffel in an oral presentation at Pitcon 2001, abstract 464.
 (23) Bard, A. J.; Fan, F. R. F.; Pierce, D. T.; Unwin, P. R.; Wipf, D. O.; Zhou, F. *Science* **1991**, *254*, 68–74.
 (24) Bard, A. J.; Fan, F. R. F.; Mirkin, M. V. In *Electroanalytical Chemistry*, Bard, A. J.; Marcel Dekker: New York, 1994; Vol. 18, p 243.
 (25) Bard, A. J.; Faulkner, L. R. *Electrochemical Methods, Fundamentals and Applications*; 2nd ed.; John Wiley & Sons: New York, 2001.
 (26) Barker, A. L.; Slevin, C. J.; Unwin, P. R.; Zhang, J. In *Surfactant Science Series*; Volkov, A. G., Ed.; Marcel Dekker: New York, 2001; Vol. 95, pp 283–324.
 (27) Unwin, P. R. *J. Chem. Soc., Faraday Trans.* **1998**, *94*, 3183–3195.
 (28) Slevin, C. J.; Unwin, P. R. *J. Am. Chem. Soc.* **2000**, *122*, 2597–2602.
 (29) Quinn, B. M.; Prieto, I.; Haram, S. K.; Bard, A. J. *J. Phys. Chem. B* **2001**, *105*, 7474–7476.
 (30) Zhang, J.; Lahtinen, R. M.; Kontturi, K.; Unwin, P. R.; Schiffrin, D. J. *Chem. Commun.* **2001**, 1818–1819.
 (31) Gyurcsanyi, R. E.; Pergel, E.; Nagy, R.; Kapui, I.; Lan, B. T. T.; Toth, K.; Bitter, I.; Lindner, E. *Anal. Chem.* **2001**, *73*, 2104–2111.
 (32) Liu, B.; Cheng, W.; Rotenberg, S. A.; Mirkin, M. V. *J. Electroanal. Chem.* **2001**, *500*, 590–597.
 (33) Gray, N. J.; Unwin, P. R. *Analyst* **2000**, *125*, 889–893.

- (34) Brust, M.; Walker, M.; Bethell, D.; Schiffrin, D. J.; Whyman, R. *Chem. Commun.* **1994**, 801–802.
 (35) Hicks, J. F.; Templeton, A. C.; Chen, S.; Sheran, K. M.; Jasti, R.; Murray, R. W.; Debord, J.; Schaaff, T. G.; Whetten, R. L. *Anal. Chem.* **1999**, *71*, 3703–3711.

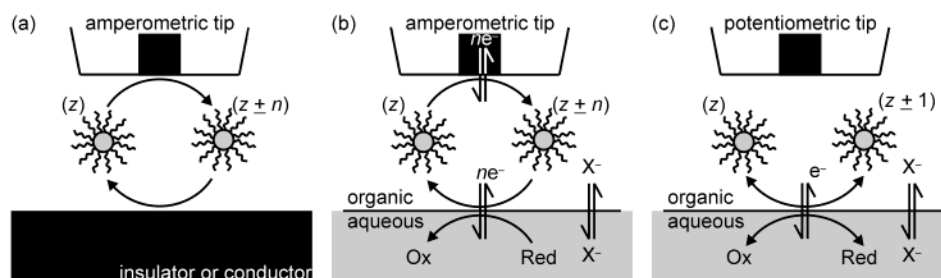


Figure 2. Schematic illustration of MPCs as SECM redox mediators: at an insulating or conducting solid substrate (a), and in an amperometric (b) or potentiometric (c) measurement at a liquid–liquid interface.

electrode and counter electrode. The working electrode used throughout was a 25 μm diameter Pt ultramicroelectrode (UME). Disk-shaped Pt SECM tips were prepared as previously described.²⁴ Briefly, Pt wire (diameter 25 μm , Goodfellows, UK) was heat-sealed in pulled borosilicate glass capillaries (Harvard GC200–10, US) under vacuum, followed by tip sharpening and polishing until the desired ratio of the overall tip radius to that of the platinum disk, R_G , was achieved. The tips used had $R_G = 5$, as determined from both optical micrographs and SECM approach curve experiments to insulating (PTFE) and conducting (Pt) substrates followed by fitting the results to the approximations provided by Amplett and Denuault.³⁶ The tip was rinsed with water, acetone, and chloroform and dried prior to each measurement.

Cell potentials were corrected to the SCE scale by the addition of ferrocene to the solution after the measurements and correlating its half-wave potential with the formal redox potential given in the literature ($E^{\text{O}'} = 0.399 \text{ V vs SCE}^{\text{37}}$). The concentration of MPC in solution could be estimated from chronoamperometric measurements at a Pt UME using the method described by Shoup and Szabo.^{25,38} The analysis of the resulting current time transients also yielded the apparent diffusion coefficient of the MPCs. This was typically $2 \times 10^{-6} \text{ cm}^2\text{s}^{-1}$, which is in good agreement with previously determined values.^{35,39}

To compare the interfacial reactivity of MPC solutions with different charge, the as-prepared MPC cores were oxidized prior to measurement using the two-phase oxidation method described by Wuelfing et al.⁷ The equilibrium potential ($E_{\text{eq}} = 0.2 \text{ V vs SCE}$) of the oxidized MPC solution was more positive by ca. 0.25 V than that of the as-prepared particles ($E_{\text{eq}} = -0.06 \text{ V vs SCE}$). However, the yields were typically very low as the oxidation method seems to be rough on the particles.

In Figure 2a, a schematic illustration of the amperometric mode of SECM operation using freely diffusing MPCs as the redox mediator is given. The MPC redox species is oxidized or reduced at the UME surface by biasing the potential to the diffusion-limiting region, generating $\text{MPC}^{z\pm n}$ where z is the charge of the MPCs in the bulk solution, and n corresponds to the number of electrons transferred to/from the metal core. The potentials were chosen from the troughs of the corresponding DPVs recorded in the same solutions. Approach curves, where the tip response is monitored as a function of distance d from the substrate under investigation, were obtained for tip approach to perfectly insulating (PTFE) and conducting (Pt) substrates.

For measurements at the liquid–liquid interface, a modified cell was used to enable the more dense 1,2-DCE phase to be used as the upper phase as described previously.⁴⁰ Electrodes were placed in the upper 1,2-DCE phase. The experimental arrangement was essentially that given in reference⁴⁰ but where the organic redox couple was replaced by the MPC solution. As the tip approaches the lower aqueous phase,

the mediator may be regenerated via interfacial bi-molecular ET depending on choice of MPC redox state and aqueous redox couple as shown schematically in Figure 2b. Kinetic information is obtained from the resulting approach curves. The SECM experiments described here were performed in feedback mode, that is, the reaction under investigation is only occurring in the vicinity of the tip and not macroscopically at the substrate. The heterogeneous ET reaction at the liquid–liquid interface is second-order but can be approximated as pseudo first-order if the concentration of one of the reactants is in excess, i.e., concentration polarization of that reactant can be neglected. For the reaction considered, this condition is only satisfied for $K_r > 20$, where $K_r = c_{\text{Red/Ox}}^{\text{w}}/c_{\text{MPC}}^{\text{o}}$.⁴¹ In all cases, the concentration of aqueous reactant was in excess compared to that of the MPC solution by at least a factor of 100.

In the potentiometric mode of operation (schematic in Figure 2c), the SECM tip is used as a redox-reference electrode. In this way, the equilibrium potential E_{eq} of the MPC solution can be monitored as the tip approaches the substrate.

The interfacial potential difference $\Delta_o^{\text{w}}\phi = \phi^{\text{w}} - \phi^{\text{o}}$ is determined by the common ion added to both phases and is given by the Nernst equation, $\Delta_o^{\text{w}}\phi = \Delta_o^{\text{w}}\phi_i^{\text{O}'} + RT/z_i F \ln(c_i^{\text{o}}/c_i^{\text{w}})$ where $\Delta_o^{\text{w}}\phi_i^{\text{O}'}$ and z represent the formal transfer potential of ion i with charge z respectively. Thus, $\Delta_o^{\text{w}}\phi$ is determined by the choice of ion and the concentrations used. The common ion is also assumed to maintain electroneutrality. Typically, ClO_4^- ($\Delta_o^{\text{w}}\phi_{\text{ClO}_4^-}^{\text{O}'} = -0.160 \text{ V}^{\text{42}}$) was used as the partitioning ion where TBAClO₄ was added to the organic phase and NaClO₄ was added to the aqueous typically at a concentration of 100 mM. Other common ions considered include the TPAS⁺ ($\Delta_o^{\text{w}}\phi_{\text{TPAS}^+}^{\text{O}'} = -0.364 \text{ V}$), TBA⁺ ($\Delta_o^{\text{w}}\phi_{\text{TBA}^+}^{\text{O}'} = -0.225 \text{ V}$) and TMA⁺ ($\Delta_o^{\text{w}}\phi_{\text{TMA}^+}^{\text{O}'} = 0.16 \text{ V}$) cations.⁴² The corresponding chloride and TPBF₂₀ salts were added to the aqueous and organic phases, respectively.

Results and Discussion

A typical example of DPV yielding a series of very regularly spaced (ΔV) peaks characteristic of QDL is given in Figure 1, where the corresponding CV is also shown. DPV peak potentials are coincident with CV half-wave potentials and can be taken as the formal redox potential $E^{\text{O}'}$ of the MPC “redox couple”.⁷ A plot of $E^{\text{O}'}$ versus MPC charge $z+n$ was linear ($R^2 > 0.999$), as expected, where z is the native charge of the MPC solution and n the number of electrons transferred (Supporting Information).³⁵ The potential of zero charge is E_{pzc} , where $z = 0$ cannot be assigned without additional information. The capacitance of the MPC can be estimated from $C = e/\Delta V = 0.62 \text{ aF}$, and this value can in turn be used to estimate the radius of the metal core $r = 0.87 \text{ nm}$ using a simple concentric sphere capacitor model.⁴ The absence of surface plasmon resonance peak in the

(36) Amplett, J. L.; Denuault, G. *J. Phys. Chem. B* **1998**, *102*, 9946–9951.

(37) Fermin, D. J.; Lahtinen, R. In *Surfactant Science Series*; Volkov, A. G., Ed.; Marcel Dekker: New York, 2001; Vol. 95, pp 179–227.

(38) Shoup, D.; Szabo, A. *J. Electroanal. Chem. Interfacial Electrochem.* **1982**, *140*, 237–245.

(39) Wuelfing, W. P.; Templeton, A. C.; Hicks, J. F.; Murray, R. W. *Anal. Chem.* **1999**, *71*, 4069–4074.

(40) Ding, Z.; Quinn, B. M.; Bard, A. J. *J. Phys. Chem. B* **2001**, *105*, 6367–6374.

(41) Barker, A. L.; Unwin, P. R.; Amemiya, S.; Zhou, J.; Bard, A. J. *J. Phys. Chem. B* **1999**, *103*, 7260–7269.

(42) Database of Gibbs Energies of Ion Transfer, <http://dcwww.epfl.ch/cgi-bin/LE/DB/InterrDB.pl>.

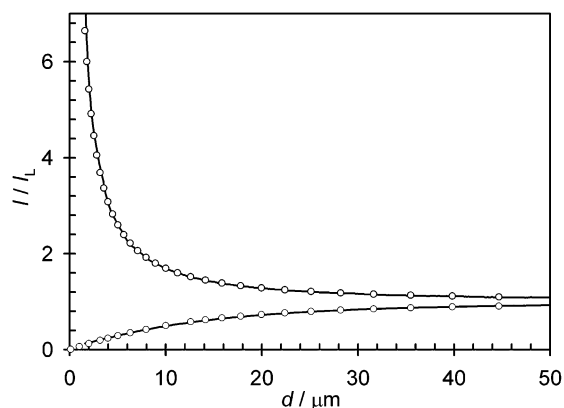
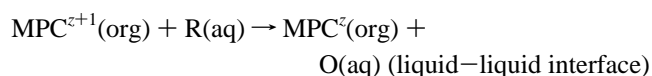


Figure 3. MPC SECM approach curves for $n = 4$ to insulating and conducting substrates giving negative (lower solid line) and positive (upper solid line) feedback respectively, where the circles are the corresponding fits to theory.

MPC solution UV–vis absorbance spectrum was consistent with particles of this size.⁴³

In Figure 3, typical examples of approach curves to insulating and conducting substrates obtained using the MPCs as redox mediators are given, where the SECM tip was biased at the diffusion-limited redox potentials for each charge-state of the MPC considered, in this case, up to 4-electron oxidation and 2-electron reduction of the particles. Approach curves to Teflon, an insulating substrate, gave negative feedback due to hindered MPC diffusion in the tip–substrate gap. These fit the theory for an approach curve to an insulator for a tip with an $R_G = 5$.³⁶ Positive feedback was noted in all cases for approaches to a Pt substrate due to mediator regeneration, in good agreement with the theory for an $R_G = 5$.³⁶ There was no difference between the responses for the different charge-states considered, illustrating that ET to the core is fast (upper detection limit for the rate constant, $k > 0.1 \text{ cm s}^{-1}$ with the tip used²⁵). These experiments demonstrate that MPCs can be used in place of traditional redox mediators in electrochemical experiments.

Subsequently, heterogeneous ET between tip generated $\text{MPC}^{z\pm n}$ in DCE and aqueous redox species was investigated. The reaction under investigation is as follows



or vice versa for interfacial oxidation where tip generated MPC^{z-1} is oxidized heterogeneously by an aqueous oxidant O .⁴⁰ The aqueous redox species considered were $\text{Ce}(\text{IV})$, $\text{Fe}(\text{CN})_6^{4-}$, $\text{Fe}(\text{CN})_6^{3-}$, $\text{Ru}(\text{NH}_3)_6^{3+}$, and $\text{Ru}(\text{CN})_6^{4-}$. The resulting approach curves either gave negative feedback which fit well with the theory for an insulator³⁶ or a more complicated response where the negative feedback was superimposed on a more gradual response, resulting from the formation of a diffusion boundary layer over few hundred micrometers from the interface. For example, approach curves to the aqueous phase reductant $\text{Fe}(\text{CN})_6^{4-}$ for tip generated $z + n$ where $n = -1, +1$ to $+4$ MPC charge states fit well to the theoretical response for an

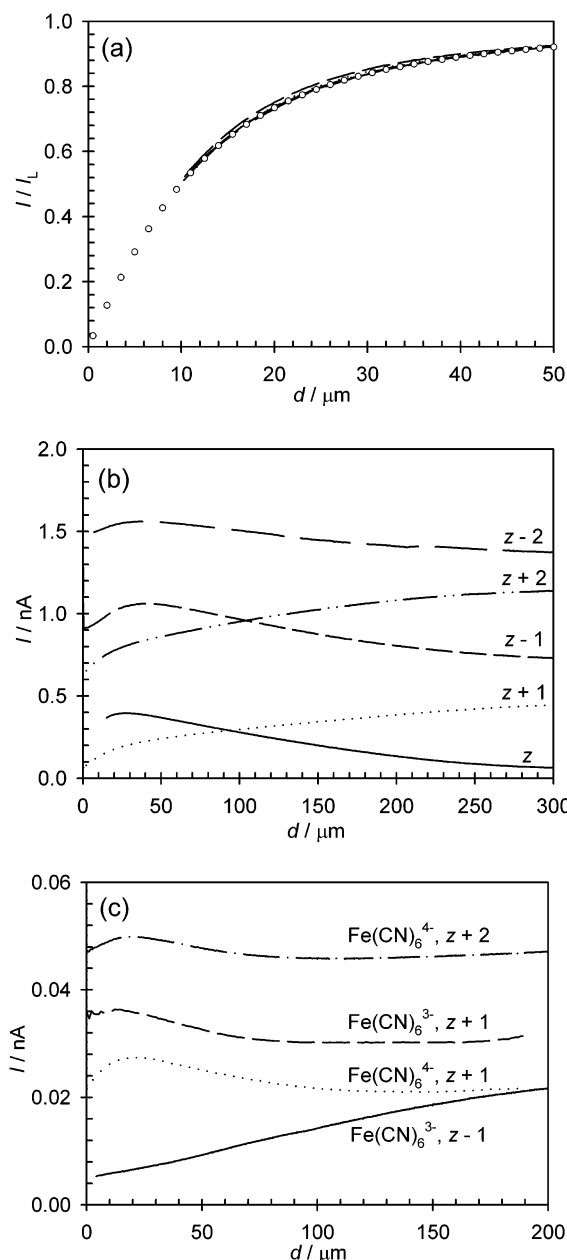


Figure 4. (a) MPC (as prepared) approach curves to an aqueous phase containing $\text{Fe}(\text{CN})_6^{4-}$ for tip generated $z + n$ for $n = -1, +1$ to $+4$ MPC charge states and theory for a perfectly insulating substrate (circles). (b) Approach curves to an aqueous phase containing $\text{Fe}(\text{CN})_6^{3-}$, where the tip generated charge state of the MPC is indicated in the figure. (c) Approach curves obtained to aqueous phase $\text{Fe}(\text{CN})_6^{4-}$ or $\text{Fe}(\text{CN})_6^{3-}$ with oxidized nanoparticles where the tip generated charge state and the aqueous phase redox species is indicated in the figure. ClO_4^- was used as the potential determining ion.

approach to an insulating substrate as shown in Figure 4a. The tip generated reduced species MPC^{z-1} is unlikely to accept electrons from the aqueous phase and the tip current should decrease due to hindered MPC^z diffusion. Thus, the negative feedback response obtained for the $z - 1$ charge-state fit was as expected. The tip generated oxidized species MPC^{z+1} was predicted to be reduced interfacially, resulting in regeneration of MPC^z in the tip substrate-gap, giving an increase in tip current. However, the response for $n = +1$ to $+4$ (all responses practically coincide) also gave negative feedback indicative of either the absence of heterogeneous ET or very slow kinetics.

(43) Hostetler, M. J.; Wingate, J. E.; Zhong, C.-J.; Harris, J. E.; Vachet, R. W.; Clark, M. R.; Londono, J. D.; Green, S. J.; Stokes, J. J.; Wignall, G. D.; Glish, G. L.; Porter, M. D.; Evans, N. D.; Murray, R. W. *Langmuir* **1998**, *14*, 17–30.

Approach curves to the other aqueous reductant considered, $\text{Ru}(\text{CN})_6^{4-}$, were identical to those for $\text{Fe}(\text{CN})_6^{4-}$ (Supporting Information).

Approach curves to aqueous oxidants typically gave more complex responses. Taking $\text{Fe}(\text{CN})_6^{3-}$ as an example, for approach curves where MPC^{z+n} is the tip-generated species, we expect a negative feedback response typical for an approach to an insulating substrate as the oxidized metal core will not donate electrons to an aqueous oxidant. However, as can be seen in Figure 4b, although the tip current did decrease as expected, the change was gradual and not localized in the tip–substrate gap. Only close to the substrate, a typical sharp decrease indicative of negative feedback was observed. For MPC^{z-n} approach curves, we expect an increase in current due to interfacial oxidation by aqueous phase $\text{Fe}(\text{CN})_6^{3-}$ regenerating MPC^z . The experimental curves did show an increase in current for $n = -1$ and -2 , but again the response was smeared out and in the vicinity of the interface, the current decreased. In a collection type experiment, where the tip was biased at E_{eq} , approach curves for the z charge-state also show a gradual increase in tip current with decreasing distance to the aqueous phase. This is a clear indication that the MPC cores are being oxidized at equilibrium by $\text{Fe}(\text{CN})_6^{3-}$ generating MPC^{z+1} , which is then rereduced at the tip resulting in the increase in current. Approach curves to the other aqueous phase oxidants considered, $\text{Ru}(\text{NH}_3)_6^{3+}$ and $\text{Ce}(\text{IV})$, showed similar trends to those obtained for $\text{Fe}(\text{CN})_6^{3-}$ (Supporting Information).

To compare the interfacial reactivity of MPC solutions with different charge, the above measurements were repeated with oxidized particles. The as prepared particles ($E_{\text{eq}} = -0.06$ V vs SCE) were oxidized in the manner described by Wuelfing et al.⁷ The resulting E_{eq} was ca. 0.25 V more positive than the as-prepared particles ($E_{\text{eq}} = 0.2$ V). From Figure 1, it can be seen that this corresponds to a change of charge state from z to $z + 1$.

Approach curves obtained to aqueous phase $\text{Fe}(\text{CN})_6^{4-}$ and $\text{Fe}(\text{CN})_6^{3-}$ are shown in Figure 4c as illustrative examples. For approaches to the aqueous oxidant $\text{Fe}(\text{CN})_6^{3-}$, the observed response was essentially as that shown in Figure 4b for more reduced particles; a gradual decrease (increase) in tip current with decreasing d for tip-generated $z - 1$ ($z + 1$). However, for approaches to the aqueous reductant $\text{Fe}(\text{CN})_6^{4-}$, it was clear that the more oxidized core could now be reduced at the interface and there were gradual changes in the tip current response consistent with an increasing concentration of reduced MPC as distance decreased. This trend is absent in Figure 4a where the equilibrium potential of the MPC solution was more negative. Similar approach curves were obtained when $\text{Ru}(\text{CN})_6^{4-}$ was used as the aqueous redox species.

In no instance, for all MPC charge-states generated at the tip (up to $2e^-$ reduction and $4e^-$ oxidation), was positive feedback obtained for approaches to any of the aqueous redox species used in this study. The driving force for heterogeneous ET at the liquid–liquid interface can be written as follows: $\Delta_{\text{o}}^{\text{w}}\phi + \Delta E^{\circ}$,⁴⁴ where $\Delta E^{\circ} = E_{\text{O/R}}^{0,\text{w}} - E_{\text{MPC}^z/\text{MPC}^{z+n}}^{0,\circ}$ is the difference in the formal potentials of the aqueous redox couple and the MPC charge state considered. Thus, for the MPC and aqueous redox couples considered here, the driving force of ET was varied by

over 1.3 V. This is sufficient to change the rate constant by several orders of magnitude from predictions based on Butler–Volmer kinetics.^{25,40} This result is unprecedented in ET studies at liquid–liquid interface—no other ET reaction to date has shown such sluggish kinetics over such a range of driving force in the absence of interfacial spacers such as adsorbed lipids. This suggests either the absence of interfacial ET or very slow kinetics ($k < 10^{-4}$ cm s⁻¹). Considering previous reports from the Murray group where two-phase oxidation of MPC solutions was reported⁷ and collection type approach curves obtained here, it can be assumed that charge can be transferred to/from the metal core interfacially. This mechanism, as opposed to reactant partitioning followed by a homogeneous ET, is further supported by the extremely hydrophobic and hydrophilic natures of the MPCs and the aqueous redox couples, respectively.

The potentiometric mode of SECM operation²⁵ offers a simple means of probing the interfacial reactivity of the MPC solution at equilibrium, i.e., without external perturbation. The equilibrium potential E_{eq} of charged MPC solutions can be written in terms of the Nernst equation, $E_{\text{eq}} = E^{\circ} + RT/F \ln[\text{MPC}^{z+1}]/[\text{MPC}^z]$, where $[\text{MPC}^{z+1}]$ and $[\text{MPC}^z]$ are the concentrations of the respective charge-states, and E° is the formal potential of the $z/z+1$ charge state. The SECM Pt UME acts as a redox reference electrode and monitors E_{eq} of the MPC “redox couple” as a function of distance to the substrate. In the absence of an interfacial reaction, the concentration ratio does not change and E_{eq} will not vary as the interface is approached.

Potentiometric approach curves are given in Figure 5 for MPC^z (a) and MPC^{z+1} (b) for tip approach to the aqueous phase in the presence and absence of redox species. $\text{Fe}(\text{CN})_6^{4-}$ and $\text{Fe}(\text{CN})_6^{3-}$ are shown for ease of comparison with amperometric approach curves given in Figure 4. For both MPC solutions, there was no change in E_{eq} in the absence of an aqueous redox species (dashed line). In the presence of $\text{Fe}(\text{CN})_6^{3-}$, E_{eq} shifts to more positive potentials as the interface is approached indicating that the particles are being oxidized. This was true for both z and $z + 1$ particles though the change in E_{eq} was greater for the z particles. MPC^{z+1} particles were reduced interfacially in the presence of aqueous $\text{Fe}(\text{CN})_6^{4-}$ and E_{eq} shifted negative in the vicinity of the interface. By contrast, for the MPC^z , there was no change in E_{eq} indicating that the aqueous $\text{Fe}(\text{CN})_6^{4-}$ cannot reduce the MPC in this valence state (under experimental conditions chosen).

The potentiometric response indicates that heterogeneous ET is dependent on core-charge and proceeds, but the reaction is not sufficiently fast to observe ET in feedback SECM mode. This is in contrast to the mass transfer limited CT response observed for the metal electrode–electrolyte interface. It is possible that although the protecting thiol layer has a negligible effect on ET kinetics at the metal–electrolyte interface, it is sufficient to depress the rate at the liquid–liquid interface. In comparison to other redox species used in ET studies at liquid–liquid interfaces, the MPC is several times larger (diameter of MPC including thiol layer is ca. 3 nm) and extremely hydrophobic. Considering investigated ET systems at liquid–liquid interfaces, fullerene is the only comparable molecule in terms of size (though still 3 times smaller), redox properties and hydrophobicity. However, in the case of C_{60} , the ET centers are not separated by the additional alkanethiol monolayer and, consequently, for the fullerene monoanion, ET at the liquid–

(44) Tsionsky, M.; Bard, A. J.; Mirkin, M. V. *J. Phys. Chem.* **1996**, *100*, 17 881–17 888.

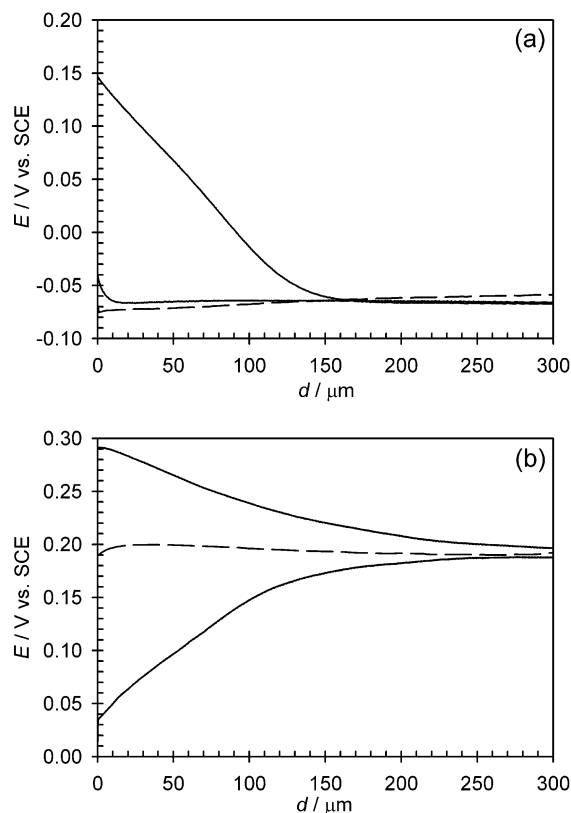


Figure 5. Potentiometric SECM approach curves (E_{eq} vs d), where the equilibrium potential of the MPC couple at the SECM electrode is monitored as a function of distance to DCE/water interface in the presence (—) and absence (---) of aqueous redox couples for (a) as prepared MPCs and (b) oxidized MPCs. The aqueous redox couple was $\text{Fe}(\text{CN})_6^{3-}$ (upper traces) and $\text{Fe}(\text{CN})_6^{4-}$ (lower traces). ClO_4^- was used as the potential determining ion.

liquid interface has been noted to occur at a measurable rate and the driving force dependence of the rate constant to be in-line with predictions based on Marcus kinetics.⁴⁵ The size and hydrophobicity may influence the distance of closest approach between the reactants at the liquid–liquid interface: considering the thickness of the interfacial layer (of the order of 10 \AA),⁴⁶ the ratio of the rate constants at liquid–liquid and metal–electrolyte can be estimated, based on the exponential relationship between the tunneling probability and distance,²⁵ to be of the order of $\exp(-\beta\Delta d)$, where β is the tunneling coefficient, and Δd is the change in tunneling distance. The tunneling coefficient has been reported to be $0.8\text{--}0.9 \text{ \AA}^{-1}$,^{7,16} and taking Δd to be 10 \AA , the ratio of the rate constant is obtained as ca. 3×10^3 . This large difference is sufficient to explain the observed differences between the rate of ET at metal–electrolyte and liquid–liquid interfaces. The charge stored on the MPC is expected to be shielded by the thiol layer⁴⁷ and as sluggish kinetics were noted for both $z + n$ and $z - n$ charge states and positively and negatively charged aqueous reactants, electrostatic repulsion is unlikely to be responsible for the low rate of electron transfer. Further study will be aimed at quantifying this effect through variation of the thickness and nature (electron density and hydrophilicity–hydrophobicity) of the protecting thiol layer.

(45) Zhang, J.; Unwin, P. R. *J. Chem. Soc., Perkin Trans. 2* **2001**, 1608–1612.

(46) Benjamin, I. *Chem. Rev.* **1996**, *96*, 1449–1475.

(47) As evidenced by the success of the simple concentric capacitor model. A more detailed picture taking into account the surrounding electrolyte solution based on the Poisson–Boltzmann equation predicts that >90% of the potential drop occurs within the thiol layer.

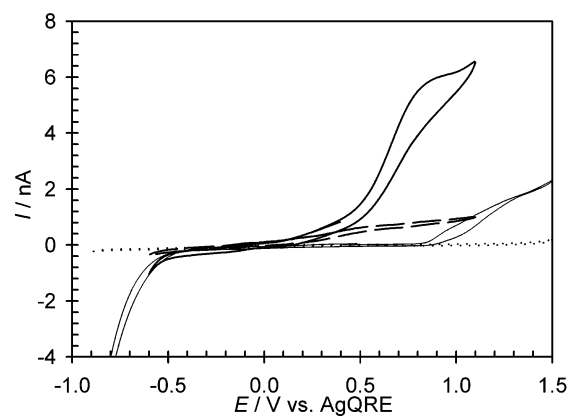


Figure 6. Cyclic voltammograms of the MPC solutions in the presence (solid line) and absence (dashed line) of the aqueous phase when TPAs^+ was used as the potential determining ion. Base electrolyte CVs in the presence (thin solid line) and absence (dotted line) of the aqueous phase are also shown.

To study the effect of $\Delta_o^w\phi$, other potential determining ions in addition to ClO_4^- were also considered. Ignoring ion association in the low permittivity DCE phase as a first approximation, for equal concentrations of the common ion added to both phases, $\Delta_o^w\phi$ is ca. -0.16 V , -0.225 , -0.365 , and $+0.16 \text{ V}$ for ClO_4^- , TBA^+ , TPAs^+ , and TMA^+ as the chosen partitioning ion, respectively. Approach curves obtained where TMA^+ was the potential determining ion were comparable to those obtained for ClO_4^- for the redox couples considered (not shown). However, when TPAs^+ or TBA^+ were used as the potential determining ions, differing results were obtained. Addition of the MPC solution to the cell, such that it was in contact with the aqueous phase containing the corresponding chloride, had an immediate effect on the CV response even when the UME was over 1 cm from the interface. Electrochemical measurements in the absence of the aqueous phase with fresh solutions gave the same response as that obtained in the presence of the other two salts TBAClO_4 and TMATPBF_{20} . CVs for the TPAsTPBF_{20} case are given in Figure 6 in the presence (solid line) and absence (dashed line) of the aqueous phase. This effect was independent of the presence or absence of the aqueous redox couple. To understand this phenomenon, CVs were also obtained in the absence of the MPC, i.e., the CV of the base window was compared in the presence and absence of the aqueous phase for the four potential determining ions considered. For both ClO_4^- and TMA^+ , the CV response was unchanged, whereas for both TPAs^+ and TBA^+ , the potential window is smaller by ca. 800 mV. CVs for the TPAsTPBF_{20} case are given in Figure 6 in the absence (dotted line) and presence of the aqueous phase (thin solid line). This effect can be rationalized in terms of electrocapillarity: the interfacial tension at the very negative potentials obtained using TPAs^+ or TBA^+ as the potential determining ion is very small and the phases mix. Due to the inverse arrangement used here with the DCE phase resting on the less dense aqueous phase, the aqueous phase “runs” through the organic phase and the potential window available at the Pt UME is limited by water oxidation and reduction. However, as can also be seen from Figure 6, this effect alone is not sufficient to explain the difference in the MPC CV response. Although a flow of water past the electrode could increase the current response due to convection, this should result in higher currents at all potentials: the currents in the negative part of the

voltammogram remain unchanged, whereas at positive potentials, the current response is amplified by ca. a factor of 10. This type of response has been observed with MPC films in aqueous solutions and was termed rectified quantized double layer charging.^{15–18} In this case, however, it is not that the negative potential response is absent but that the positive potential response is greatly enhanced. We propose that due to the variable dielectric environment, the MPCs partly precipitate on the electrode surface, and the film undergoes rectified QDL due to the presence of hydrophobic anions. This response is superimposed on the QDL response from the solution species. This type of electrochemically induced microemulsification/mixing presents a novel environment combining properties of both solvents.

Conclusions

The use of monolayer-protected clusters as redox mediators in scanning electrochemical microscopy experiments has been demonstrated. They can be used as tunable electrochemical reactants whereby the charge of the species and the energy available for the reaction can be altered via the oxidation state of the MPC.

Electron transfer reactions involving MPCs have been investigated both at conventional metal–electrolyte as well as at electrified liquid–liquid interfaces. At metal electrodes, the rate of electron transfer is fast (rate constant $> 0.1 \text{ cm s}^{-1}$), whereas it was found to be surprisingly low at the water–dichloroethane interface. However, ET was observed to depend on the charge of MPCs and the aqueous redox species. The low rate of ET was rationalized in terms of the large size and

hydrophobicity of the MPCs resulting in a large separation between the reactant of heterogeneous ET across a liquid–liquid interface.

The interfacial potential difference was altered by the use of potential determining ions. This resulted in spontaneous mixing of the phases in the cases of TPAs⁺ and TBA⁺ cations and the electrochemical response observed was a superposition of ET from the solution species and rectified QDL originating from a nanoparticle film formed due to modified dielectric properties of the solvent environment.

The use of SECM in both amperometric and potentiometric modes presents a versatile tool for probing the local concentration and flux of the electroactive species. This technique together with the modification of the nanoparticle properties via changing the nature of the protecting layer (the electron density and hydrophilicity) forms a powerful combination to spatially resolved electrochemical detection with chemically tunable redox mediators.

Acknowledgment. The authors are grateful to Santosh K. Haram and Zhifeng Ding for valuable discussion. Research funding provided by the National Technology Agency, Finland and The Academy of Finland is gratefully acknowledged.

Supporting Information Available: Additional experimental results (DPV peak potentials vs the nanoparticle charge and SECM approach curves). This material is available free of charge via the Internet at <http://pubs.acs.org>.

JA0282137